

Photoinduced Electron Transfer in Covalently Linked 1,8-Naphthalimide/Viologen Systems

Thao P. Le, Joy E. Rogers, and Lisa A. Kelly*

*Department of Chemistry and Biochemistry, University of Maryland, Baltimore County, 1000 Hilltop Circle, Baltimore, Maryland 21250**Received: March 3, 2000; In Final Form: May 18, 2000*

A series of polymethylene-linked 1,8-naphthalimide/viologen diads has been synthesized. The number of intervening methylenes was varied from 2 to 6. For comparison, a series of *N*-alkylpyridiniumyl-1,8-naphthalimide “parent” compounds was prepared and photophysically characterized. Relative to the parent compounds, the electronically excited singlet state of the 1,8-naphthalimide was found to be quenched by the covalently attached viologen. From Stern–Volmer analyses of the steady-state fluorescence spectra, along with the singlet-state lifetime of the pyridinium-substituted 1,8-naphthalimide, the rate constants for intramolecular quenching were calculated to range from $1.5 \times 10^{10} \text{ s}^{-1}$ (2 intervening methylenes) to $8.3 \times 10^7 \text{ s}^{-1}$ (6 intervening methylenes) in aqueous buffered solution. For comparison, the intermolecular reactivity of the excited singlet state of *N*-alkylpyridiniumyl-1,8-naphthalimides with methylviologen was assessed. In 0.5 M phosphate buffer (pH 7.0), the bimolecular rate constant was found to be $3.2 \times 10^9 \text{ M}^{-1} \text{ s}^{-1}$. Nanosecond laser flash photolysis studies were carried out to identify the quenching products. From these studies, reduced methylviologen was identified as a singlet-state quenching product. From these results, we attribute both the intra- and intermolecular quenching process to electron transfer from the singlet excited state of 1,8-naphthalimide to methylviologen. Within the covalently linked series, the rate constant for intramolecular electron transfer was found to vary exponentially with the number of intervening methylenes. Linear least-squares analysis of the results yielded an apparent β value of 1.04 \AA^{-1} for electron transfer through the polymethylene bridge.

Introduction

Photoinduced electron transfer plays a key role in light-driven chemical, physical, and biological processes. Photosynthesis represents a noteworthy and ubiquitous model that has motivated the design of many elaborate assemblies to convert light energy into chemical potential. To mimic the charge transfer processes that accompany photosynthesis, covalently linked arrays of electron donors and acceptors are often used.^{1,2} From these synthetic assemblies, the effects of thermodynamic driving force, distance and intervening medium on electron transfer (ET) kinetics have been investigated. To best understand the distance dependence, electron donor–acceptor systems that are linked by rigid spacing groups have been investigated. Specifically, the rate constant (k_{ET}) for ET through steroidal,³ norbornyl,⁴ or peptide⁵ spacers has shown to decrease exponentially with the distance (r_{DA}) between the donor and acceptor group according to $k_{\text{ET}} = A \exp(-\beta(r_{\text{DA}} - r_{\text{DA}}^0))$. In this treatment, β depends on the nature of the linkage or intervening medium and r_{DA}^0 is the distance of closest approach.

Donor–acceptor systems linked by flexible spacing groups, such as polymethylene chains ($-(\text{CH}_2)_n-$), are generally easier to synthesize. However, extracting linkage-dependent β values from these systems is complicated by the fact that electron transfer may occur from all conformers in solution.⁶ To overcome this difficulty, cyclodextrins capable of forming inclusion complexes with flexible, covalently linked donor–acceptor systems have been used to force the assembly into an

extended conformation.^{7–10} In a series of naphthoxyl- $(\text{CH}_2)_n$ -viologen donor–acceptor diads, exponential distance dependences were observed at shorter distances ($n \leq 6$).⁷ For the longer linkages, the nonexponential behavior was corrected by complexation with cyclodextrin. In a separate study, rate constants for electron transfer from the MLCT excited state of a tris(2,2'-bipyridyl)ruthenium(II) complex to a covalently attached viologen were measured as a function of the number of intervening methylenes.⁸ In aqueous solution, exponential distance dependence up to six methylenes was observed. The nonlinearities at longer separation distances were corrected by encapsulating the diad in β -cyclodextrin. Although conformational flexibility is certainly a complication in extracting distance dependencies through polymethylene chains, these reports suggest that photophysical perturbations, due to through-space interactions, occur primarily at longer separation distances.

In this paper, we characterize the intramolecular electron transfer kinetics in a series of donor–acceptor diads in which a 1,8-naphthalimide chromophore is covalently attached to a viologen electron acceptor. The electron donor and acceptor are separated by 2–6 intervening methylenes. From the kinetic data, polymethylene distance dependencies are extracted. For comparison, intermolecular electron transfer from the naphthalimide singlet excited state to methylviologen was also investigated. The viologens are ubiquitous electron acceptors and have been coupled to tris(bipyridyl)ruthenium(II) chromophores^{8,11} and porphyrins,^{12–15} to study intramolecular electron transfer. Likewise, the facile and reversible one-electron reduction of *N*-substituted 1,8-naphthalimides has been studied electrochemi-

* Corresponding author: E-mail: lkelly@umbc.edu.

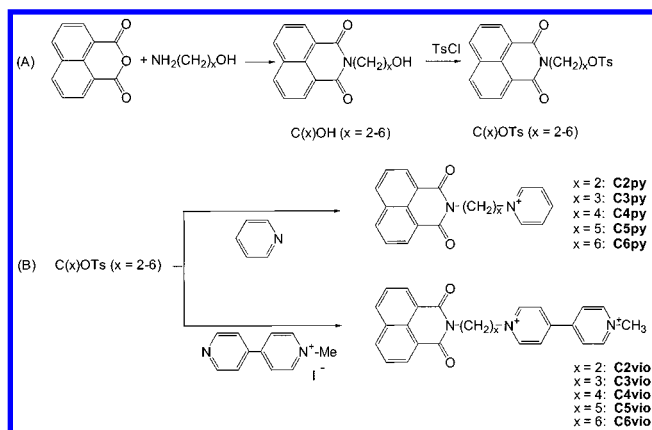


Figure 1. Synthesis of pyridinium-substituted derivatives of 1,8-naphthalimide (**C2py**, **C3py**, **C4py**, **C5py**, and **C6py**) and donor–acceptor diad systems (**C2vio**, **C3vio**, **C4vio**, **C5vio**, and **C6vio**) used in this study.

cally.¹⁶ Following photon absorption, the electronically excited singlet and triplet states of these aromatic imides have been used to oxidize DNA nucleotides and duplex DNA.^{17,18} In a separate report, intramolecular electron transfer to the excited singlet and triplet states of *N*-substituted 1,8-naphthalimide from aniline or methoxyaniline has been demonstrated.¹⁹ Thus, both constituents of the naphthalimide–viologen diads are generally employed as electron acceptors. In this work, we demonstrate photoinduced electron transfer from the singlet excited state of 1,8-naphthalimide to the covalently attached viologen and demonstrate the versatile reactivity of naphthalimide excited states as reducing agents in photoinduced electron transfer.

Experimental Section

Materials. 1,8-Naphthalic anhydride (97%, Acros) was recrystallized twice from *N,N*-dimethylacetamide (DMA) and dried in vacuo prior to use. 2-Amino-1-ethanol (Aldrich, 99+%), 3-amino-1-propanol (Acros, 99%), 4-amino-1-butanol (Acros, 98%), 5-amino-1-propanol (Acros, 97%), and 6-amino-1-hexanol (Acros, 94%) were used as received. 4,4'-Dipyridyl (99.8%), *p*-toluenesulfonyl chloride (99+%), and methyl iodide (99%) were obtained from Aldrich and used as received. Tetrabutylammonium perchlorate (TBAP) (99%) was obtained from Sigma and dried in vacuo prior to use. Anhydrous pyridine was obtained from Aldrich and used as received. Spectral grade acetonitrile (Fluka) was used as received for electrochemical studies. Methylviologen (dichloride hydrate, 98%) was obtained from Aldrich and recrystallized from ethanol prior to use. Elemental analyses were performed by Atlantic Microlabs.

The functionalized naphthalimide compounds used in this study were synthesized as shown in Figure 1. All of the pyridinium-substituted 1,8-naphthalimides were isolated and used as their monochloride salts. The viologen-linked diads were isolated and used as diiodide salts as described below. The compounds within the series are named according to the number of methylene substituents (x) between the naphthalene imide chromophore and the covalently linked pyridinium (**Cxpy**) or viologen (**Cxvio**).

***N*-(2-(*N*-Pyridiniumyl)ethyl)-1,8-naphthalenimide (**C2py**).** 1,8-Naphthalic anhydride (25 mmol) was suspended in 40 mL of DMA. 1-Amino-2-ethanol (50 mmol) was added dropwise to the suspension over 30 min. The mixture was stirred at 100 °C for 3 h. After removal of the solvent on a rotary evaporator, water (ca. 25 mL) was added to the residue. The resulting white precipitate (*N*-(2-ethanol)-1,8-naphthalenimide (**C2OH**)) was

filtered and dried (yield = 81%). The pyridinium-substituted imide was prepared by dissolving **C2OH** (1.5 g) and 1.4 g of *p*-toluenesulfonyl chloride (1.4 g) in 4 mL of dry pyridine and stirring at room temperature for 12 h. The precipitate that was formed was collected by vacuum filtration, dissolved in a minimal amount of water and stirred with DOWEX 1 \times 8 200 ion-exchange resin for ca. 30 min to obtain the chloride salt of **C2py**. The DOWEX resin was filtered from solution and the water removed from the filtrate. The resulting product was recrystallized twice in methanol under an atmosphere of diethyl ether. The product was obtained in 60% yield after recrystallization. Analytically pure material was obtained by further purification on a neutral alumina column. Trace impurities were removed by elution with methanol. The product was then eluted from the column using 50:50 H_2O :methanol. ^1H NMR ($\text{DMSO}-d_6$): 9.20 (d, 2H, pyr), 8.60 (t, 1H, pyr), 8.50 (d, 2H, naphth), 8.41 (d, 2H, naphth), 8.09 (t, 2H, pyr), 7.86 (t, 2H, naphth), 4.96 (t, 2H, CH_2), 4.61 (t, 2H, CH_2). Anal. Calcd ($\text{C}_{19}\text{H}_{15}\text{N}_2\text{O}_2\text{Cl}$): C, 67.36; H, 4.46; N, 8.27. Found: C, 67.02; H, 4.48; N, 8.04.

***N*-(3-(*N*-Pyridiniumyl)propyl)-1,8-naphthalenimide (**C3py**).** The synthetic and purification procedures were identical to those used for **C2py**. The material was obtained in 45% overall yield after recrystallization from methanol. ^1H NMR ($\text{DMSO}-d_6$): 9.11 (d, 2H, pyr), 8.56 (t, 1H, pyr), 8.40 (d+d, 4H, naphth), 8.11 (t, 2H, pyr), 7.86 (t, 2H, naphth), 4.68 (t, 2H, CH_2), 4.12 (t, 2H, CH_2), 2.30 (m, 2H, CH_2). Anal. Calcd ($\text{C}_{20}\text{H}_{17}\text{N}_2\text{O}_2\text{Cl} \cdot 2\text{H}_2\text{O}$): C, 61.78; H, 4.41; N, 7.20. Found: C, 61.85; H, 4.01; N, 7.20.

***N*-(4-(*N*-Pyridiniumyl)butyl)-1,8-naphthalenimide (**C4py**).** The *N*-butanol intermediate (*N*-(4-butanol)-1,8-naphthalenimide (**C4OH**)) was prepared in 91% yield using the procedure described above for **C2OH**. The dried product was stirred under nitrogen at room temperature for 12 h with 1.2 equiv of *p*-toluenesulfonyl chloride in a minimal amount of dry pyridine. **C4py** was precipitated from the pyridine by the addition of THF and converted to the chloride salt as described above. The material was dried and purified on a neutral alumina column. After elution of the impurities with methanol, the desired product was eluted from the column using 30:70 H_2O :methanol. The material was recrystallized from methanol in an atmosphere of diethyl ether (yield = 40%). ^1H NMR ($\text{DMSO}-d_6$): 9.11 (d, 2H, pyr), 8.56 (t, 1H, pyr), 8.47 (dd, 4H, naphth), 8.14 (t, 2H, pyr), 7.87 (t, 2H, naphth), 4.64 (t, 2H, CH_2), 4.09 (t, 2H, CH_2), 2.02 (m, 2H, CH_2), 1.67 (m, 2H, CH_2). Anal. Calcd ($\text{C}_{21}\text{H}_{19}\text{N}_2\text{O}_2\text{Cl} \cdot 2\text{H}_2\text{O}$): C, 62.61; H, 4.75; N, 6.95. Found: C, 62.54; H, 4.81; N, 6.93.

***N*-(5-(*N*-Pyridiniumyl)pentyl)-1,8-naphthalenimide (**C5py**).** The synthetic and purification procedures were identical to those used for **C4py**. **C5py** was obtained in 83% yield from the alcohol precursor. ^1H NMR ($\text{DMSO}-d_6$): 9.07 (d, 2H, pyr), 8.56 (t, 1H, pyr), 8.45 (dd, 4H, naphth), 8.12 (t, 2H, pyr), 7.84 (t, 2H, naphth), 4.58 (t, 2H, CH_2), 4.01 (t, 2H, CH_2), 1.95 (m, 2H, CH_2), 1.65 (m, 2H, CH_2), 1.33 (m, 2H, CH_2). Anal. Calcd ($\text{C}_{22}\text{H}_{21}\text{N}_2\text{O}_2\text{Cl} \cdot \text{H}_2\text{O}$): C, 66.24; H, 5.31; N, 7.02. Found: C, 66.08; H, 5.56; N, 6.95.

***N*-(6-(*N*-Pyridiniumyl)hexyl)-1,8-naphthalenimide (**C6py**).** 1-Amino-6-hexanol (34 mmol) in 20 mL of DMA was added dropwise, over a period of 30 min, to a suspension of 1,8-naphthalic anhydride (17 mmol) in 250 mL of DMA. The mixture was stirred at 100 °C for 6 h. After removal of the solvent on a rotary evaporator, water (ca. 100 mL) was added to the residue. The resulting white precipitate (*N*-(6-hexanol)-1,8-naphthalenimide (**C6OH**)) was filtered and dried (yield =

72%). The pyridinium-substituted imide was prepared by dissolving **C6OH** (1.50 g) and 1.4 g of *p*-toluenesulfonyl chloride (1.15 g) in 4 mL of dry pyridine and stirring at room temperature for 4 h. The product (precipitated as the chloride salt) was obtained in 72% yield and was purified by recrystallization from methanol/acetonitrile. ¹H NMR (DMSO-*d*₆): 9.12 (d, 2H, pyr), 8.59 (t, 1H, pyr), 8.47 (dd, 4H, naphth), 8.15 (t, 2H, pyr), 7.86 (t, 2H, pyr), 4.61 (t, 2H, CH₂), 4.02 (t, 2H, CH₂), 1.95 (m, 2H, CH₂), 1.63 (m, 2H, CH₂), 1.36 (m, 4H, CH₂).

N-Methyl-*N'*-ethyl-4,4'-bipyridiniumyl-1,8-naphthalimide (**C2vio**). **C2OH** (6.1 mmol) was dissolved in 12 mL of dry pyridine. One equivalent of tosyl chloride was added, and the mixture was stirred at 0 °C for 2 h. The white powder was filtered and washed with cold pyridine to yield 40% of the tosylated intermediate (**C2OTs**). **C2OTs** (2.0 mmol) and 1-methyl-4,4'-bipyridinium (prepared as previously described)²⁰ (1.6 mmol) were refluxed in CH₃CN (20 mL) for 15 h. The iodide salt was isolated as a red-orange precipitate that was filtered and washed with a minimum amount of cold acetonitrile to yield 79% **C2vio**. Analytically pure product was obtained after successive (five times) recrystallizations from methanol. ¹H NMR (DMSO-*d*₆): (**C2OTs**) 8.43 (dd, 4H, naphth), 7.84 (t, 2H, naphth), 7.45 (d, 2H, ts), 6.83 (d, 2H, ts), 4.32 (m, 4H, CH₂), 2.45 (s, 3H, CH₃). ¹H NMR (DMSO-*d*₆): (**C2vio**) 9.53 (d, 2H, vio), 9.28 (d, 2H, vio), 8.76 (dd, 4H, vio), 8.51 (d, 2H, naphth), 8.39 (d, 2H, naphth), 7.87 (t, 2H, naphth), 5.04 (t, 2H, CH₂), 4.68 (t, 2H), 4.42 (s, 3H, -CH₃). Anal. Calcd (C₂₅H₂₁N₃O₂I₂·2H₂O): C, 43.44; H, 3.06; N, 6.08. Found: C, 43.80; H, 3.09; N, 6.14.

N-Methyl-*N'*-propyl-4,4'-bipyridiniumyl-1,8-naphthalimide (**C3vio**). **C3OTs** was prepared as described above for **C2OTs**. The product was isolated by the addition of cold water to the pyridine solution and vacuum filtration of the water insoluble product. **C3vio** was prepared by refluxing **C3OTs** with 1.2 equiv of the iodide salt of *N*-methyl-4,4'-bipyridinium in a minimal amount of CH₃CN for 12 h. The red-orange precipitate that was formed was filtered and washed with cold acetonitrile to yield **C3vio**. The product was twice recrystallized from methanol (yield = 13%). ¹H NMR (DMSO-*d*₆): (**C3OTs**) 8.43 (dd, 4H, naphth), 7.85 (t, 2H, naphth), 7.67 (d, 2H, ts), 7.35 (d, 2H, ts), 4.11 (m, 4H, CH₂), 2.34 (s, 3H, CH₃), 1.9 (m, 2H, CH₂). ¹H NMR (DMSO-*d*₆): (**C3vio**) 9.38 (d, 2H, vio), 9.27 (d, 2H, vio), 8.77 (dd, 4H, vio), 8.52 (dd, 4H, naphth), 7.91 (t, 2H, naph), 4.82 (t, 2H, CH₂), 4.43 (s, 3H, CH₃), 4.21 (t, 2H, CH₂), 2.39 (m, 2H, CH₂). Anal. Calcd (C₂₆H₂₃N₃O₂I₂): C, 46.66; H, 3.46; N, 6.28. Found: C, 46.97; H, 3.44; N, 6.23.

N-Methyl-*N'*-butyl-4,4'-bipyridiniumyl-1,8-naphthalimide (**C4vio**) and *N*-Methyl-*N'*-pentyl-4,4'-bipyridiniumyl-1,8-naphthalimide (**C5vio**). **C4vio** and **C5vio** were prepared as the diiodide salts using procedures identical to those described above. Analytically pure material was obtained after recrystallization from methanol four times. ¹H NMR (DMSO-*d*₆): (**C4OTs**) 8.41 (dd, 4H, naphth), 7.81 (t, 2H, naphth), 7.72 (d, 2H, ts), 7.36 (d, 2H, ts), 4.01 (m, 4H, CH₂), 2.29 (s, 3H, CH₃), 1.57 (m, 4H, CH₂). ¹H NMR (DMSO-*d*₆): (**C4vio**) 9.39 (d, 2H, vio), 9.29 (d, 2H, vio), 8.77 (dd, 4H, vio), 8.54 (dd, 4H, naphth), 7.92 (t, 2H, naphth), 4.75 (t, 2H, CH₂), 4.47 (s, 3H, CH₃), 4.16 (m, 2H, CH₂), 2.11 (m, 2H, CH₂), 1.75 (m, 2H, CH₂). Anal. Calcd (C₂₇H₂₅N₃O₂I₂·2H₂O): C, 46.24; H, 3.59; N, 5.99. Found: C, 46.58; H, 3.79; N, 6.04. ¹H NMR (DMSO-*d*₆): (**C5OTs**) 8.41 (d, 4H, naphth), 7.81 (t, 2H, naphth), 7.39 (d, 2H, ts), 6.84 (d, 2H, ts), 4.35 (t, 2H, CH₂), 4.21 (t, 2H, CH₂), 2.29 (s, 3H, CH₃), 1.93 (m, 6H, CH₂). ¹H NMR (DMSO-*d*₆): (**C5vio**) 9.39 (d, 2H, vio), 9.31 (d, 2H, vio), 8.79 (dd, 4H, vio), 8.49 (dd, 4H, naphth),

7.91 (t, 2H, naphth), 4.72 (t, 2H, CH₂), 4.57 (s, 2H, CH₃), 4.09 (t, 2H, CH₂), 2.08 (m, 2H, CH₂), 1.74 (m, 2H, CH₂), 1.43 (m, 2H, CH₂). Anal. Calcd (C₂₈H₂₇N₃O₂I₂·2H₂O): C, 45.86; H, 3.71; N, 5.73. Found: C, 45.70; H, 3.81; N, 5.62.

N-Methyl-*N'*-hexyl-4,4'-bipyridiniumyl-1,8-naphthalimide (**C6vio**). Alcohol (**C6OH**, 5.05 mmol) was dissolved in pyridine (4 mL) at room temperature. *p*-Toluenesulfonyl chloride (6.06 mmol) was added in the solution, and the mixture was stirred at room temperature for 3 h. The white precipitate that formed was filtered and washed with cold water to yield 63% **C6OTs**. **C6OTs** (1.1 mmol) was refluxed with an equimolar amount of 1-methyl-4,4'-bipyridinium in 10 mL of CH₃CN overnight. The red-orange precipitate that was formed was filtered and washed with minimum amount of cold acetonitrile (yield = 38%). The product was recrystallized two times from methanol. ¹H NMR (DMSO-*d*₆): (**C6OTs**) 8.42 (dd, 4H, naphth), 7.82 (t, 2H, naphth), 7.73 (d, 2H, ts), 7.42 (d, 2H, ts), 3.96 (m, 4H, CH₂), 3.28 (s, 3H, CH₃), 1.52 (m, 4H, CH₂), 1.22 (m, 4H, CH₂). ¹H NMR (DMSO-*d*₆): (**C6vio**) 9.37 (d, 2H, vio), 9.28 (d, 2H, vio), 8.76 (dd, 4H, vio), 8.47 (dd, 4H, naphth), 7.87 (t, 2H, naphth), 4.69 (t, 2H, CH₂), 4.04 (t, 2H, CH₂), 4.43 (s, 3H, CH₃), 1.97 (m, 2H, CH₂), 1.64 (m, 2H, CH₂), 1.38 (m, 4H, CH₂). Anal. Calcd (C₂₉H₂₉N₃O₂I₂): C, 48.96; H, 4.11; N, 5.91. Found: C, 49.45; H, 4.13; N, 5.79.

General Techniques. Ground-state UV/vis absorption spectra were measured using a JASCO V-570 double-beam spectrophotometer. Proton NMR spectra were obtained using either a GE QE-300 or a Varian Mercury 200 MHz NMR spectrometer. Fluorescence spectra were measured using a SPEX Fluoromax-2 fluorescence spectrometer.

Fluorescence lifetimes were measured using time-correlated single-photon counting techniques at the National Synchrotron Light Source. Excitation light from the quartz-windowed, bending magnet port of beamline U9B was monochromated and used for pulsed excitation of the sample. The temporal (with respect to the excitation pulse) and spectral properties of the emitted light were simultaneously detected using a resistive-anode, single-photon counting detector. The optical configuration and detection system have been previously described.²¹ For these experiments, 344 nm excitation light was employed. Fluorescence from the sample, integrated from 370 to 500 nm, was deconvoluted with the measured instrument response function to obtain the singlet state lifetimes of the systems.

One-electron reduction potentials of the naphthalene imide derivatives were measured in anhydrous acetonitrile containing ca. 2.5 mM imide and 0.10 M tetrabutylammonium perchlorate (TBAP) as a supporting electrolyte. Solutions were bubbled with nitrogen prior to measurement. The cyclic voltammograms were obtained using a BAS CV-1B CV controller that was interfaced to a pentium PC for data acquisition. For these measurements, platinum working and counter electrodes were employed, with a silver/silver chloride (approximately 3 M KCl) reference electrode. A scan rate of 200 mV/s was employed. For reference, the half-wave potential of a 5 mM ferrocene solution was measured and determined to be 0.443 V vs Ag/AgCl with the electrode system employed.

Nanosecond transient absorption measurements were carried out using 355 nm excitation. A detailed description of the laser flash photolysis apparatus has been previously published.²²

Results

A series of donor-acceptor diad systems (**C2vio**–**C6vio**), containing 1,8-naphthalimide covalently attached to 4,4'-bipy-

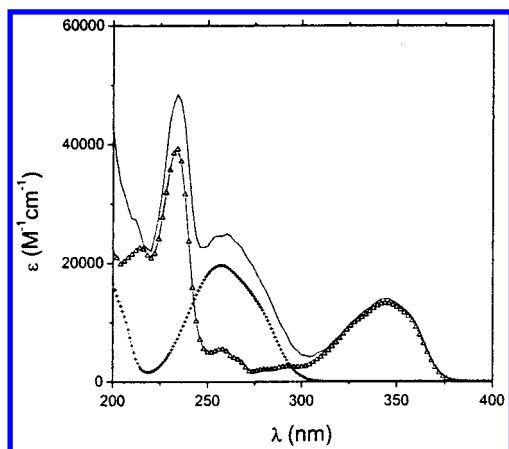


Figure 2. Ground-state UV absorption spectrum of **C3py** (triangles), methylviologen (crosses), and **C3vio** (solid line, no symbol) measured in phosphate buffer (10 mM; pH 7.0).

ridinium, was prepared as shown in Figure 1. The separation distance between the two components was varied by increasing the number of methylene spacers. The analogous series (**C2py**–**C6py**) was synthesized as water-soluble “model” compounds to be used in the photophysical studies.

Ground-State Spectral and Redox Studies. The UV spectra of **C3py** and **C3vio** are shown in Figure 2. The ground-state spectra of the other compounds (**C2py**–**C6py**) within the series are identical. Likewise, the spectral properties of the naphthalimide-viologen diads (**C2vio**–**C6vio**) do not vary with the number of intervening methylene units (data not shown). As shown in Figure 2, the ground-state absorption spectra of the covalently linked donor–acceptor systems is adequately described as the sum of the 1,8-naphthalimide and viologen parts. Specifically, there are no spectral perturbations in the 344 nm absorption band of the naphthalimide moiety upon covalent attachment of the viologen. Moreover, the additional absorption intensity of **C3vio** relative to **C3py**, in the 200–300 nm range, is attributed to the presence of 4,4'-bipyridinium.²³ Thus, the spectra indicate no evidence of electronic interaction in the ground state.

The redox properties of the compounds were characterized by cyclic voltammetry. Voltammograms of **C3py** and **C3vio** are shown in Figure 3a,b, respectively. In both cases, the oxidation and reduction waves are completely reversible. From Figure 3a, a single reduction wave was observed. The half-wave potential ($E_{1/2}$), taken as the midpoint of the cathodic and anodic peak potentials, was determined to be -1.30 V vs Ag/AgCl. At more negative potentials, solvent reduction occurs. In Figure 3b, three reduction waves ($E_{1/2} = -0.39$, -0.83 , and -1.32 V vs Ag/AgCl) are apparent. Within each of the series, the half-wave potentials are identical within experimental error (± 10 mV). From the data shown in Figure 3, we assign the reversible process occurring at -1.32 V as the one-electron reduction of the naphthalimide moiety. This is nearly identical to that reported for an uncharged 1,8-naphthalimide derivative.^{22,24} By virtue of their absence in Figure 3a, we assign the -0.39 and -0.83 V reduction waves to two successive viologen-centered reduction processes. The reversible and successive single electron reductions of viologen dications in aqueous solution are known ($E_{1/2}^0 = -0.45$ and -0.88 V vs NHE)²⁵ and are virtually identical to the viologen-centered reductions of **C3vio**.²⁶ No redox processes were observed up to a potential of 2.0 V, where solvent oxidation began to occur.

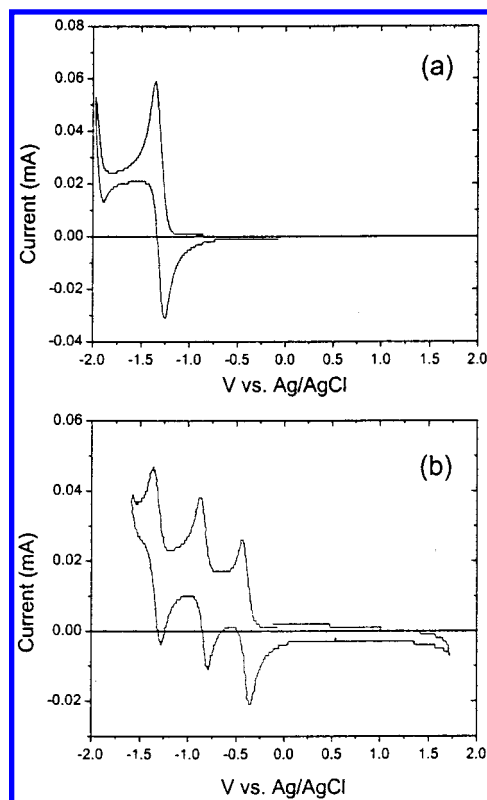


Figure 3. Cyclic voltammograms of (a) **C3py** and (b) **C3vio** measured in acetonitrile (0.10 M TBAP) vs Ag/AgCl (3 M KCl).

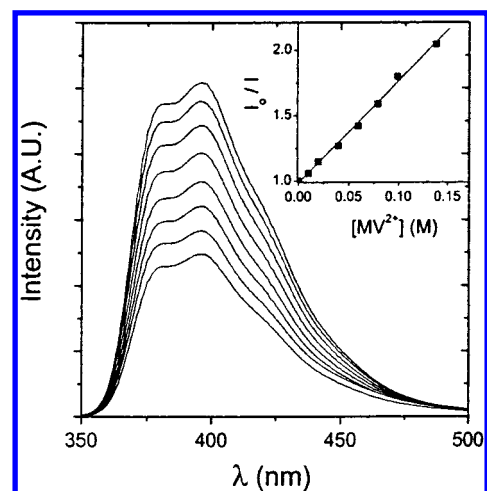


Figure 4. Stern–Volmer quenching (fluorescence and inset of plot) of **C3py** by MV^{2+} . $[MV^{2+}] = 0, 9.85, 19.7, 39.4, 59.1, 78.8, 98.5, 137$ mM. All spectra were obtained in 0.5 M sodium phosphate buffer (pH 7.0) using an excitation wavelength of 344 nm.

Bimolecular Quenching of Naphthalimide Singlet Excited States. As shown in Figure 4, the addition of methylviologen to an aqueous solution of **C3py** results in quenching of the naphthalimide fluorescence. Since the quenching process is a diffusional one between two cationic species, a sufficiently high buffer concentration (0.5 M sodium phosphate, pH 7.0) was used to maintain a constant ionic strength of the solution as methylviologen is added. At the highest methylviologen concentration employed (ca. 0.1 M), the ground-state absorption spectrum of the naphthalimide was unperturbed and showed no evidence of complex formation. The ratio of the integrated fluorescence intensities before and after the addition of methylviologen (I_0/I) was fit to eq 1. Linear regression analysis of the data shown in the inset of Figure 4 yielded a Stern–Volmer

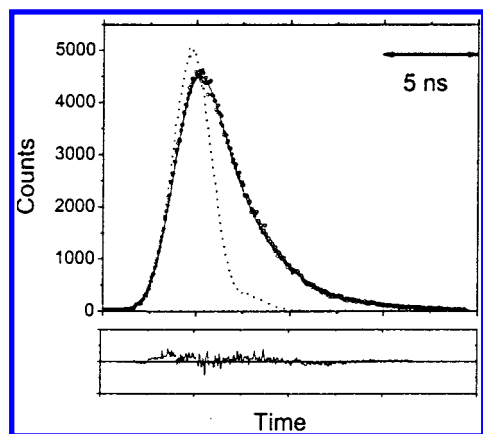


Figure 5. Fluorescence decay of ${}^1\text{C3py}^*$ ($5\ \mu\text{M}$ in $10\ \text{mM}$ pH 7.0 phosphate buffer) measured by time-correlated single-photon counting. The instrument response function (dashed line) is shown, along with the best reconvoluted fit of the data. An excitation wavelength of 344 nm was employed. The integrated emission between 370 and 500 nm is shown.

constant (K_{SV}) of $7.80\ \text{M}^{-1}$.

$$\frac{I_0}{I} = 1 + K_{\text{SV}}[\text{MV}^{2+}] \quad (1)$$

Singlet-State Lifetimes. The singlet-state lifetime of one of the pyridinium-substituted 1,8-naphthalimides was measured using single-photon counting techniques. The fluorescence decay of ${}^1\text{C3py}^*$ is shown in Figure 5, along with the instrument response of the system. The decay is adequately fit to a single-exponential decay model. From reconvolution analysis of this decay, we estimate the lifetime of the S_1 state to be $2.46 \pm 0.20\ \text{ns}$. This lifetime is nearly identical to a lifetime of 2.4 ns for the decay of the $\text{S}_1\text{--S}_n$ absorption in picosecond pump-probe experiments.²² Lifetime measurements of the other compounds within the series were not made. However, since the relative fluorescence quantum yields of **C2py**–**C6py** were identical, it is reasonable to assume that the five compounds have the same singlet-state lifetime.

From the measured singlet state lifetime, along with the Stern–Volmer quenching results shown in Figure 4, a bimolecular rate constant of $3.2 \times 10^9\ \text{M}^{-1}\ \text{s}^{-1}$ is obtained for quenching of the naphthalimide singlet excited state by methylviologen in aqueous buffered solution. The mechanism of quenching is addressed below.

Intramolecular Quenching of Naphthalimide Excited Singlet States. Shown in Figure 6 (top spectrum) is the fluorescence emission spectrum of **C3py** measured in buffered aqueous solution. Using solutions of matched optical density at 344 nm (the excitation wavelength), the emission spectra were recorded for the other compounds in the pyridinium-substituted 1,8-naphthalimide series. Both the spectral shape and intensities were identical to the top spectrum shown in Figure 4. For each pair of “model” and viologen-linked compounds (**C2py** and **C2vio**, **C3py** and **C3vio**, **C4py** and **C4vio**, **C5py** and **C5vio**, **C6py** and **C6vio**), fluorescence emission spectra were acquired. Within each pair, the optical densities at the excitation wavelength were matched. Since the fluorescence quantum efficiencies were identical for each member of the pyridinium-linked naphthalimide series, the intensities of the “model” compounds were used to normalize the data within the series. The combined data are shown in Figure 6. Apparent from Figure 6, the covalent attachment of the 4,4′-bipyridinium moiety diminishes the

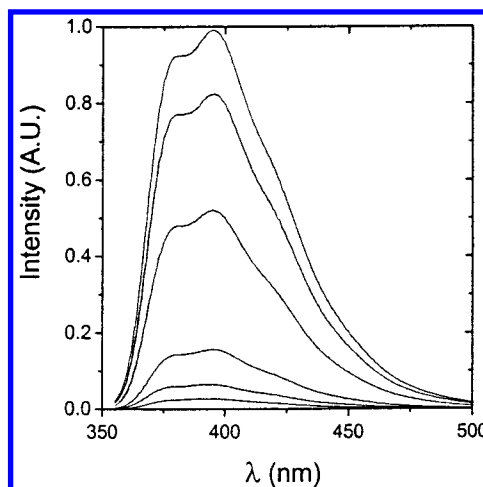


Figure 6. Steady-state fluorescence spectra, of **C3py** (top, solid line), **C6vio**, **C5vio**, **C4vio**, **C3vio**, and **C2vio** (in order of decreasing intensities). Spectra were recorded using solutions of matched optical densities at 344 nm in $10\ \text{mM}$ phosphate buffer (pH 7.0).

fluorescence intensity. However, the identical fluorescence spectral features shown in Figures 4 and 6 suggests that there is no electronic perturbation of naphthalimide by the covalently attached viologen. The magnitude of the fluorescence quenching increases with decreasing naphthalimide–viologen separation distance. The mechanisms of inter- and intramolecular quenching by methylviologen, along with the distance-dependent fluorescence quenching in the covalently linked systems, are discussed below.

Discussion

Mechanisms of Inter- and Intramolecular Quenching.

From the data shown in Figure 4, it is apparent that the methylviologen dication quenches the singlet excited state of the pyridinium-functionalized 1,8-naphthalimides. When the viologen and naphthalimide moieties are covalently attached, quenching of the singlet excited state of the naphthalimide by the 4,4′-bipyridinium also occurs. In both cases, we consider two mechanisms of reactivity: (i) singlet–singlet energy transfer from the electronically excited naphthalimide to methylviologen and (ii) photoinduced electron transfer. The UV absorption spectrum of methylviologen is well-known, and has a long-wavelength onset of $<350\ \text{nm}$.²³ Fluorescence of the naphthalene imide chromophores used in this study is observed only at wavelengths longer than 350 nm (Figures 4 and 6). Since there is no spectral overlap between the viologen absorption spectrum and naphthalimide fluorescence spectrum, we conclude that energy transfer from the S_1 state of naphthalimide to methylviologen is thermodynamically uphill and is not a likely quenching pathway. We thus consider electron transfer quenching processes.

It is known that both methylviologen and 1,8-naphthalimide species can act as electron acceptors. The one-electron reduction potential of methylviologen ($E_{1/2}^0 = -0.450\ \text{V}$ vs NHE)²⁷ is more positive than that of naphthalimide ($E_{1/2}^0 = -1.26\ \text{V}$ vs SCE).¹⁶ There have been no published reports of viologen or 1,8-naphthalimide as electron donors in photoinduced charge transfer processes. The oxidation potential of 4-amino-1,8-naphthalimide ($1.20\ \text{V}$ vs SCE) has been reported.²⁸ However, oxidation of this chromophore is largely centered on the amine substituent. This is supported by the fact that, in this chromophore, the lowest excited singlet state is largely charge transfer (amine to aromatic amide) in nature.^{29,30}

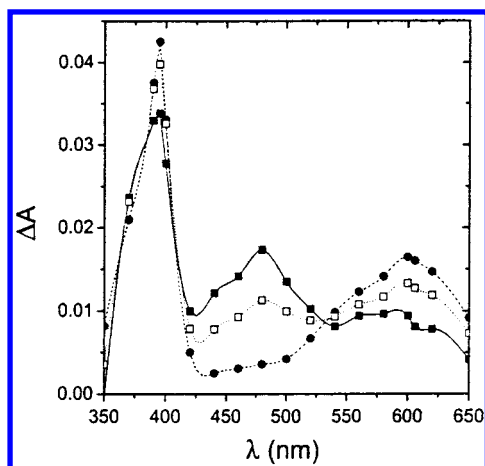


Figure 7. Transient absorption spectrum obtained upon 355 nm pulsed excitation of **C2py** (9 μ M) in the presence of 0.33 M methylviologen in argon-saturated aqueous solution containing 0.50 M phosphate buffer (pH 7.0). Spectra were recorded 0 (■), 12 (□), and 70 (●) μ s after excitation.

The cyclic voltammograms measured in this study did not reveal any oxidation processes up to 2.0 eV. Clearly, one of the diad components must act as an electron donor for a photoinduced electron transfer quenching mechanism to be operative.

To elucidate the mechanism of singlet-state quenching, laser flash photolysis experiments were carried out to identify the quenching products. Shown in Figure 7 is the transient absorption spectrum observed upon pulsed 355 nm excitation of **C2py** in the presence of methylviologen. Under the conditions employed, 72% of the **C2py** singlet states were quenched by methylviologen and all of the light is absorbed by the naphthalimide chromophore. Immediately after the 8 ns laser pulse, spectral features characteristic of both viologen radical cation (395 and 600 nm)²³ are superimposed with the T_1 – T_n naphthalimide excited state ($\lambda_{\text{max}} = 480$ nm).¹⁸ Since the spectral features of the singlet-derived product are consistent with production of viologen radical cation, we conclude that quenching of the naphthalimide singlet excited state is via electron transfer to methylviologen (eq 2a).



From the spectra, we estimate the efficiency of production of solvent-separated redox products $k_{\text{sep}}/(k_{\text{sep}} + k_{\text{rec}})$ to be 12%. On longer time scales, additional viologen radical cation is produced from quenching of the triplet state.

By analogy with the intermolecular quenching products observed, we attribute fluorescence quenching of naphthalimide by the covalently attached viologen to electron transfer. No significant amounts of long-lived intramolecular quenching products were observed on time scales longer than 10 ns. However, in all cases, a small and reproducible absorption feature at 395 nm, characteristic of the viologen radical cation, is seen in the spectra.

Energetics of Electron Transfer. Neglecting solvation of the charge transfer products relative to the reactants, the thermodynamic driving force for electron transfer from the singlet excited state of naphthalimide (NI) to methylviologen

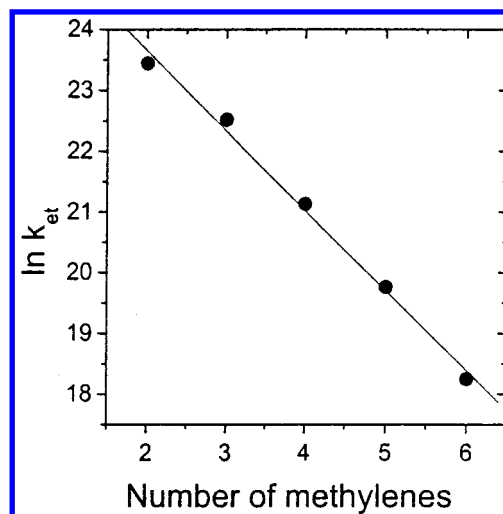


Figure 8. Rate constants for intramolecular electron transfer plotted according to eq 6. Rate constants were evaluated using data from Figures 5 and 6, along with eq 4 ($k_{\text{et}} = 1.5 \times 10^{10} \text{ s}^{-1}$, $6.0 \times 10^9 \text{ s}^{-1}$, $1.5 \times 10^9 \text{ s}^{-1}$, $3.8 \times 10^8 \text{ s}^{-1}$, and $8.3 \times 10^7 \text{ s}^{-1}$ for **C2py**–**C6py**).

(V) is given by eq 3

$$\Delta G^\circ = -(E_{1/2}(\text{V}^{2+}/\text{V}^{\bullet+}) - E_{1/2}(\text{NI}^{\bullet+}/\text{NI})) - E_{00} \quad (3)$$

where E_{00} is the singlet-state energy of the naphthalimide chromophore. The S_1 energy of N-substituted 1,8-naphthalimide has been determined by ourselves and others to be in the range 3.4–3.5 eV.^{22,31} Using $E_{00} = 3.4$ eV, along with the $\text{V}^{2+}/\text{V}^{\bullet+}$ half-wave potential of -0.39 V vs Ag/AgCl measured in this work, it is apparent that exergonic electron transfer will occur when the oxidation potential ($E_{1/2}(\text{NI}^{\bullet+}/\text{NI})$) is less than ca. 3.0 eV. Solvent oxidation precludes measuring potentials greater than 2.0 eV (Figure 3). Thus, it is not surprising that the oxidation wave was not observed but that photoinduced electron transfer from methylviologen to the naphthalimide excited state does occur.

Distance Dependence of Electron Transfer Rates. From the singlet-state lifetimes of the “parent” naphthalimide compounds (**C2py**–**C6py**), along with the steady-state fluorescence spectra shown in Figure 6, the rate constants for intramolecular electron transfer were calculated (eq 4).

$$\frac{I_o}{I} = 1 + \frac{k_{\text{ET}}}{k_d} \quad (4)$$

In eq 4, I_o and I are the integrated fluorescence intensities for each pair of “parent” and viologen-linked compounds, respectively. The intramolecular electron transfer rate constants, k_{ET} , was evaluated using the known singlet-state lifetimes of the “parent” **Cxvio** compounds ($k_d = 1/\tau_d = 4.1 \times 10^8 \text{ s}^{-1}$).³² The rate constants are given in Figure 8.

As shown in Figure 8, the rate constants vary exponentially with the number of intervening methylenes. In a classical treatment, k_{ET} is related to the electronic coupling matrix element between donor and acceptor ($|V|$), the Gibbs free energy change for the electron transfer step (ΔG°), and the sum of the molecular (λ_i) and solvent (λ_s) reorganization energies ($\lambda = \lambda_i + \lambda_s$) according to eq 5.³³

$$k_{\text{ET}} = \left(\frac{2|V|^2}{h} \right) \left(\frac{\pi^3}{\lambda RT} \right)^{1/2} \exp \left(\frac{-(\Delta G^\circ + \lambda)^2}{4\lambda RT} \right) \quad (5)$$

The $|V|^2$ term decreases exponentially with distance (eq 6), where β describes the efficiency of the intervening medium to conduct the electron and r_{DA} is the donor/acceptor separation distance.

$$|V|^2 \propto \exp(-\beta(r_{\text{DA}} - r_{\text{DA}}^0)) \quad (6)$$

The exponential distance dependence of k_{ET} shown in Figure 8 supports an electron transfer mechanism involving superexchange through the polymethylene spacer. From a linear regression analysis of the data shown in Figure 8, the β value was calculated to be 1.32 per methylene or 1.04 \AA^{-1} (assuming 1.27 \AA per methylene).³⁴ The fact that k_{ET} decays exponentially over the range of distances provided by 2–6 methylenes suggests that conformation has a relatively small effect on k_{ET} . Yonemoto et al. have studied the intramolecular electron transfer kinetics in covalently linked tris(bipyridyl)ruthenium(II)/viologen systems.⁸ In this work, exponential distance dependences up to 6-methylene linkages were observed, suggesting that the kinetics are conformation-independent. In the tris(bipyridyl)ruthenium(II)/viologen systems, an apparent β value (uncorrected for solvent reorganization energies) of 1.38 \AA^{-1} was obtained for forward electron transfer in acetonitrile. For longer linkages (7–8 methylenes), rate constants deviated from the predicted distance dependence, suggesting that an additional ET pathway is provided by through-space interactions. For these longer-chain systems, complexation by β -cyclodextrin brought the kinetic data points back onto the predicted line.⁸ In a separate study, Park et al. demonstrated exponential distance dependences for electron transfer in aqueous solutions of covalently linked naphthoxyl/viologen donor/acceptor systems.⁷ In this study, an apparent β value of 0.86 \AA^{-1} was obtained in aqueous solution. Thus, our observation of predominantly an exponential decrease in k_{ET} with distance (Figure 8), coupled with previously published reports, suggests that through-space interactions between the electron donor and acceptor, via conformational flexibility of the polymethylene linkage, have little effect on the electron transfer process. Although the apparent β value of 1.04 \AA^{-1} obtained in our polymethylene-linked naphthalimide/viologen diads is not identical to those reported previously,^{7,8} it is in the range (1.38 – 0.86 \AA^{-1}) of those observed for other donor/acceptor systems.

In conclusion, we have demonstrated singlet state quenching of N-substituted 1,8-naphthalimide by methylviologen. The transient absorption spectrum of the intermolecular electron transfer products is consistent with production of reduced methylviologen, suggesting that photooxidation of the naphthalimide excited state is occurring. When the electron donor and acceptor are covalently linked by a series of 2–6 methylene spacers, a linkage-dependent quenching occurs. The rate constant for electron transfer decays exponentially with distance, consistent with electron transfer mediated by the polymethylene bridge. From the results, an apparent β of 1.04 \AA^{-1} is obtained.

Acknowledgment. This work is supported by the American Cancer Society, Maryland Division.

References and Notes

- Wasielowski, M. R. *Chem. Rev.* **1992**, *92*, 435–461.
- Gust, D.; Moore, T. A.; Moore, A. L. *Acc. Chem. Res.* **1993**, *26*, 198–205.
- Closs, G. L.; Miller, J. R. *Science* **1988**, *240*, 440–447.
- Warman, J. M.; Smit, K. J.; de Haas, M. P.; Jonker, S. A.; Paddon-Row, M. N.; Oliver, A. M.; Kroon, J.; Oevering, H.; Verhoeven, J. W. *J. Phys. Chem.* **1991**, *95*, 1979–1987. Paddon-Row, M. N.; Oliver, A. M.; Warman, J. M.; Smit, K. J.; de Haas, M. P.; Oevering, H.; Verhoeven, J. W. *J. Phys. Chem.* **1988**, *92*, 6958–6962. Oliver, A. M.; Craig, D. C.; Paddon-Row, M. N.; Kroon, J.; Verhoeven, J. W. *Chem. Phys. Lett.* **1988**, *150*, 366–373.
- Jones, G.; Lu, L. N.; Fu, H.; Farahat, C. W.; Oh, C.; Greenfield, S. R.; Gosztola, D. J.; Wasielewski, M. R. *J. Phys. Chem. B* **1999**, *103*, 572–581. Mishra, A. K.; Chandrasekar, R.; Faraggi, M.; Klapper, M. H. *J. Am. Chem. Soc.* **1994**, *116*, 1414–1422. Isied, S. S.; Ogawa, M. Y.; Wishart, J. F. *Chem. Rev.* **1992**, *92*, 381–394.
- Siemiarz, A.; McIntosh, A. R.; Ho, T. F.; Stillman, M. J.; Roach, K. J.; Weedon, A. C.; Bolton, J. R.; Connolly, J. S. *J. Am. Chem. Soc.* **1983**, *105*, 7224–7230. Mataga, N.; Karen, A.; Okada, T.; Nishitani, S.; Kurata, N.; Sakada, Y.; Misumi, S. *J. Phys. Chem.* **1984**, *88*, 5138–5141.
- Park, J. W.; Lee, B. A.; Lee, S. Y. *J. Phys. Chem. B* **1998**, *102*, 8209–8215.
- Yonemoto, E. H.; Saupe, G. B.; Schmehl, R. H.; Hubig, S. M.; Riley, R. L.; Iverson, B. L.; Mallouk, T. E. *J. Am. Chem. Soc.* **1994**, *116*, 4786–4795.
- Yonemura, H.; Kasahara, M.; Saito, H.; Nakamura, H.; Matsuo, T. *J. Phys. Chem.* **1992**, *96*, 5765–5770. Yonemura, H.; Norjiri, T.; Matsuo, T. *Chem. Lett.* **1994**, 2097–2100.
- Toki, A.; Yonemura, H.; Matsuo, T. *Bull. Chem. Soc. Jpn.* **1993**, *66*, 3382. Yonemura, H.; Nakamura, H.; Matsuo, T. *Chem. Phys. Lett.* **1989**, *155*, 157–161. Yonemura, H.; Nakamura, H.; Matsuo, T. *Chem. Phys.* **1992**, *162*, 69–78.
- Yonemoto, E. H.; Kim, Y.; Schmehl, R. H.; Wallin, J. O.; Shoulders, B. A.; Richardson, B. R.; Haw, J. F.; Mallouk, T. E. *J. Am. Chem. Soc.* **1994**, *116*, 10557–10563.
- Dupuis, B.; Michaut, C.; Jouanin, I.; Delaire, J.; Robin, P.; Fenevrou, P.; Dentan, V. *Chem. Phys. Lett.* **1999**, *300*, 169–176.
- Batteas, J. D.; Harriman, A.; Kanda, Y.; Mataga, N.; Nowak, A. K. *J. Am. Chem. Soc.* **1990**, *112*, 126–133.
- Harriman, A.; Porter, G.; Wilowska, A. *J. Chem. Soc., Faraday Trans. 2* **1984**, *80*, 191–204.
- Noda, S.; Hosono, H.; Okura, I.; Yamamoto, Y.; Inoue, Y. *J. Photochem. Photobiol., A: Chem.* **1990**, *53*, 423–429. Noda, S.; Hosono, H.; Okura, I.; Yamamoto, Y.; Inoue, Y. *J. Chem. Soc., Faraday Trans.* **1990**, *86*, 811–814.
- Viehbeck, A.; Goldberg, M. J.; Kovac, C. A. *J. Electrochem. Soc.* **1990**, *137*, 1460–1466.
- Saito, I.; Takayama, M.; Sugiyama, H.; Nakatani, K. *J. Am. Chem. Soc.* **1995**, *117*, 6406–6407. Saito, I.; Takayama, M. *J. Am. Chem. Soc.* **1995**, *117*, 5590–5591.
- Rogers, J. E.; Weiss, S. J.; Kelly, L. A. *J. Am. Chem. Soc.* **2000**, *122*, 427–436.
- Van Dijk, S. I.; Groen, C. P.; Hartl, F.; Brouwer, A. M.; Verhoeven, J. W. *J. Am. Chem. Soc.* **1996**, *118*, 8425–8532.
- Kelly, L. A.; Rodgers, M. A. J. *J. Phys. Chem.* **1994**, *98*, 6386–6391.
- Kelly, L. A.; Trunk, J. G.; Polewski, K.; Sutherland, J. C. *Rev. Sci. Instrum.* **1995**, *66*, 1496–1498. Kelly, L. A.; Trunk, J. G.; Sutherland, J. C. *Rev. Sci. Instrum.* **1997**, *68*, 2279–2286.
- Rogers, J. E.; Kelly, L. A. *J. Am. Chem. Soc.* **1999**, *121*, 3854–3861.
- Watanabe, T.; Honda, K. *J. Phys. Chem.* **1982**, *86*, 2617–2619.
- The Fc^+/Fc redox couple has been measured in acetonitrile: $E_{1/2}^0 = 0.69 \text{ V}$ vs NHE (Barrette, W.; Johnson, H.; Sawyer, D. *Anal. Chem.* **1984**, *56*, 1890). Using this value, along with the measured Fc^+/Fc half-wave potential in this work (0.43 V vs Ag/AgCl), the half-wave potential for the naphthalimide-centered reduction in **C3vio** is computed to be -1.07 V vs NHE in acetonitrile. This is nearly identical to the value published in ref 22 ($E_{1/2}^0 = -1.01 \text{ V}$ vs NHE).
- Bird, C. L.; Kuhn, A. T. *Chem. Soc. Rev.* **1981**, *10*, 49–82.
- Using $E_{1/2}^0 = 0.40 \text{ V}$ vs NHE for the Fc^+/Fc couple in aqueous solution (Sawyer, D. T.; Sobkowiak, A.; Roberts, J. I. *Electrochemistry for Chemists*, 2nd ed.; Wiley-Interscience: New York, 1995; p 203), along with our measured half-wave potential for the ferrocene/ferrocenium couple (0.43 V vs Ag/AgCl), we estimate the viologen-centered reductions to be -0.42 and -0.86 V vs NHE.
- Wardman, P. *J. Phys. Chem. Ref. Data* **1989**, *18*, 1637–1723.
- Greenfield, S. R.; Svec, W. A.; Gosztola, D.; Wasielewski, M. R. *J. Am. Chem. Soc.* **1996**, *118*, 6767–6777.
- DeSilva, A. P.; Gunaratne, H. Q. N.; Habib-Jiwan, J.-L.; McCoy, C. P.; Rice, T. E.; Soumillion, J.-P. *Angew. Chem., Int. Ed. Engl.* **1995**, *34*, 1728–1731.
- Korol'kova, N. V.; Val'kova, G. A.; Shigorin, D. N.; Shigalevskii, V. A.; Vostrova, V. N. *Russ. J. Phys. Chem.* **1990**, *64*, 206–209.
- Wintgens, V.; Valet, P.; Kossanyi, J.; Biczok, L.; Demeter, A.; Berces, T. *J. Chem. Soc., Faraday Trans.* **1994**, *90*, 411–422. Aveline, B. M.; Matsugo, S.; Redmond, R. W. *J. Am. Chem. Soc.* **1997**, *119*, 11785–11795.

(32) The fluorescence lifetime was measured for **C3py** (Figure 5). Since the fluorescence quantum yields of **C2py**–**C6py** were identical, a singlet-state lifetime of 2.46 ns was used for all of the compounds within the **Cxpy** series.

(33) Newton, M. D.; Sutin, N. *Annu. Rev. Phys. Chem.* **1984**, 35, 437–480. Marcus, R. A.; Sutin, N. *Biochim. Biophys. Acta* **1985**, 811, 265–322. Marcus, R. A. *J. Chem. Phys.* **1965**, 43, 679–701.

(34) The distance dependence is referred to as an “apparent” β since it neglects solvent reorganization energies (λ_s). Solvent reorganization energies have been calculated for electron donor/acceptor systems separated by 1–5 and 7 or 8 methylene units (ref 11). If the donor and acceptor are considered as hard spheres 3.1 Å radii, λ_s were found to range from 1.08 to 1.23 Å for spheres separated by 2–5 methylenes. Thus, it is assumed that deviation from the predicted exponential dependence (eq 5) is negligible.